Exposure to per- and polyfluoroalkyl substances and high-throughput proteomics in Hispanic youth

Jiawen Carmen Chen[a,*], Jesse A. Goodrich[a], Douglas I. Walker[b], Jiawen Liao[a], Elizabeth Costello[a], Tanya L. Alderete[c], Damaskini Valvi[b], Hailey Hampson[a], Shiwen Li[a], Brittney O. Baumert[a], Sarah Rock[a], Dean P. Jones[d], Sandrah P. Eckel[a], Rob McConnell[a], Frank D. Gilliland[a], Max T. Aung[a], David V. Conti[a], Zhanghua Chen[a], Lida Chatzi[a]

[a]Department of Population and Public Health Sciences, University of Southern California Keck School of Medicine, Los Angeles, CA, United States

[b]Department of Environmental Medicine and Public Health, Icahn School of Medicine at Mount Sinai, New York, NY, United States

[c]Department of Integrative Physiology, University of Colorado Boulder, Boulder, CO, United States

[d]Clinical Biomarkers Laboratory, Division of Pulmonary, Allergy, Critical Care and Sleep Medicine, Emory University, Atlanta, GA, United States

Abstract

Background: Strong epidemiological evidence shows positive associations between exposure to per- and polyfluoroalkyl substances (PFAS) and adverse cardiometabolic outcomes (e.g., diabetes, hypertension, and dyslipidemia). However, the underlying cardiometabolic-relevant biological activities of PFAS in humans remain largely unclear.

*Corresponding author at: Department of Population and Public Health Sciences, University of Southern California Keck School of Medicine, 1845 N Soto St, Los Angeles, CA 90032, United States. chenjiaw@usc.edu (J.C. Chen).

Aim: We evaluated the associations of PFAS exposure with high-throughput proteomics in Hispanic youth.

Material and Methods: We included 312 overweight/obese adolescents from the Study of Latino Adolescents at Risk (SOLAR) between 2001 and 2012, along with 137 young adults from the Metabolic and Asthma Incidence Research (Meta-AIR) between 2014 and 2018. Plasma PFAS (i.e., PFOS, PFOA, PFHxS, PFHpS, PFNA) were quantified using liquid-chromatography high-resolution mass spectrometry. Plasma proteins ($n = 334$) were measured utilizing the proximity extension assay using an Olink Explore Cardiometabolic Panel I. We conducted linear regression with covariate adjustment to identify PFAS-associated proteins. Ingenuity Pathway Analysis, protein-protein interaction network analysis, and protein annotation were used to investigate alterations in biological functions and protein clusters.

Results: Results after adjusting for multiple comparisons showed 13 significant PFAS-associated proteins in SOLAR and six in Meta-AIR, sharing similar functions in inflammation, immunity, and oxidative stress. In SOLAR, PFNA demonstrated significant positive associations with the largest number of proteins, including ACP5, CLEC1A, HMOX1, LRP11, MCAM, SPARCL1, and SSC5D. After considering the mixture effect of PFAS, only SSC5D remained significant. In Meta-AIR, PFAS mixtures showed positive associations with GDF15 and IL6. Exploratory analysis showed similar findings. Specifically, pathway analysis in SOLAR showed PFOA- and PFNA-associated activation of immune-related pathways, and PFNA-associated activation of inflammatory response. In Meta-AIR, PFHxS-associated activation of dendric cell maturation was found. Moreover, PFAS was associated with common protein clusters of immunoregulatory interactions and JAK-STAT signaling in both cohorts.

Conclusion: PFAS was associated with broad alterations of the proteomic profiles linked to pro-inflammation and immunoregulation. The biological functions of these proteins provide insight into potential molecular mechanisms of PFAS toxicity.

1. Introduction

Per- and polyfluoroalkyl substances (PFAS) are a group of synthetic organic chemicals that have raised significant concerns due to their remarkable resistance to biological and environmental degradation, as well as their ability to bioaccumulate in the environment (Cousins et al., 2019; Kissa, 2001). Over 97 % of the US population have measurable perfluorooctanoic acid (PFOA), perfluorooctanesulfonic acid (PFOS), perfluorohexanesulfonic acid (PFHxS), and perfluorononanoic acid (PFNA) in blood according to the National Health and Nutrition Examination Survey (NHANES) data from 2005 to 2018 (Calafat et al., 2019; Lewis et al., 2015; Sun et al., 2024). The detrimental effects of PFAS exposure on human health have been extensively documented in numerous systematic reviews and *meta*-analyses, particularly on cardiometabolic health, such as diabetes (Gui et al., 2023), hypertension (Pan et al., 2023), dyslipidemia (Liu et al., 2023), and non-alcoholic fatty liver disease (Costello et al., 2022). According

to a study conducted among 1.3 million adults with overweight or obesity in the US in 2012–2013, over 80 % of the participants had at least one cardiometabolic risk factor, including elevated blood pressure, elevated triglycerides, low high-density lipoprotein cholesterol, and prediabetes (Karhunen et al., 2023). Therefore, understanding the underlying cardiometabolic mechanisms relevant to PFAS is crucial for the development of preventive strategies and targeted interventions against cardiometabolic outcomes.

Prior in vitro and in vivo animal research has helped elucidate the mechanisms of PFAS toxicity on cardiometabolic health. One prominent mechanism involves peroxisome proliferator-activated receptors (PPARs) (Evans et al., 2022). PPARs, as fatty acid sensors, regulate the formation, utilization, and metabolism of lipids and glucose throughout the body, thereby contributing to the pathophysiology of various cardiometabolic health conditions, such as disrupted glucose and lipid homeostasis, metabolic disorder, and inflammation (Attema et al., 2022; Kirk et al., 2021; Szilagyi et al., 2020; Wagner and Wagner, 2020). Additionally, PFAS impact Ca^{2+} signaling, nuclear factor kappa B (NF-κB) modulation, oxidative stress, and cytokine levels (Ehrlich et al., 2023), where these biological processes are emerging mechanisms in cardiometabolic health (Dubois-Deruy et al., 2020; Fiordelisi et al., 2019; Ghigo et al., 2017; Karhunen et al., 2023). However, to understand the potential cardiometabolic mechanistic changes observed in the human body in relation to PFAS exposure, comprehensive epidemiological studies are needed to explore the molecular signatures of PFAS in humans.

Omics technologies have emerged as a valuable tool in environmental epidemiology, enabling the identification of cellular-level biological signatures of environmental exposure and facilitating the development of plausible physiological mechanisms (Kyrtopoulos, 2013). Particularly, proteomic profiles provide crucial information about variations in the relative abundance, induction, and repression of thousands of proteins (Guo et al., 2021). Proteomic data serve to potentially unveil the biological functions, metabolic networks, and functional protein interaction networks of cells and organisms at a systemic level in response to an environmental exposure (Guo et al., 2021). Hence, functional proteins altered by environmental stressors can be selected as novel biomarkers to assess the toxicity of environmental stressors, the presence of specific compounds, and the progression of pollutant accumulation.

Despite significant advancements, the use of high-throughput proteomics in environmental epidemiology is still a developing field. To date, only a limited number of studies have investigated the connection between PFAS exposure and proteomic biomarkers to elucidate the molecular features of potential PFAS mechanistic toxicity, such as inflammation, cellular metabolism, and endocrine disruption. Two recent proteomic studies on Swedish middle-aged (Salihovic et al., 2020) and older-aged populations (Dunder et al., 2023) have evaluated associations of PFAS with 86 inflammatory proteins and 249 proteins linked to inflammation, metabolism, and cardiovascular disease using Olink high-throughput technique, respectively. They found that PFAS exposure was linked to alterations of proteomic profiles, such as reduced inflammation. However, these two proteomics studies focus on the Swedish population with relatively older age groups, leaving a gap in research on young populations from diverse ethnic backgrounds that are historically underrepresented

in biomedical research. Furthermore, the scope of these studies is limited as they only examined individual PFAS congeners, whereas humans are exposed to a mixture of correlated PFAS compounds, potentially resulting in synergistic health effects.

In our study, we aim to investigate the associations of five individual PFAS congeners and their mixtures with a high-throughput panel of cardiometabolic proteins using Olink. Olink utilizes a novel proximity extension assay technology, which has been validated for technical robustness, demonstrating good reproducibility and stability across multiple studies (Carlyle et al., 2022; Haslam et al., 2022). Our study included baseline data from (1) the Study of Latino Adolescents at Risk (SOLAR), comprising of Hispanic overweight or obese children, as well as data from (2) the Metabolic and Asthma Incidence Research (Meta-AIR), comprising of young adults with a history of childhood overweight or obesity. Childhood and adolescence are crucial developmental stages for cellular differentiation and the formation of metabolic tissues (Casazza et al., 2008; Kelly et al., 2011). Obesity during these periods contributes to an increased risk of cardiometabolic diseases and cause-specific mortality in adulthood (Chung et al., 2018). Consequently, investigating PFAS exposure in populations during these sensitive developmental phases, particularly those with a high metabolic risk, is imperative.

By using two independent cohorts of adolescents and young adults with high body mass index (BMI), we aim to identify PFAS-associated cardiometabolic relevant proteins and alterations of novel biological processes, as well as evaluate the persistence of these associations from adolescence to adulthood. Our findings have significance for early detection of PFAS-associated cardiometabolic risk and targeted disease prevention and intervention, as well as provide further molecular insights into the adverse effects of PFAS on cardiometabolic outcomes. In addition, our emphasis on Hispanic populations in the US, an understudied group in biomedical research, contributes to a better biological understanding of PFAS in human health across ethnic backgrounds.

2. Methods

2.1. Study populations

2.1.1. Study of Latino Adolescents at Risk (SOLAR)—This study was conducted using the baseline data from the SOLAR (5R01 DK 059211) cohort (Alderete et al., 2017). A total of 328 overweight or obese children between 8 and 13 years old were recruited in two waves between 2001 and 2012 (Goodrich et al., 2023). Participants underwent annual clinical visits at the University of Southern California (USC) General Clinical Research Center or Clinical Trials Unit. Inclusion criteria were direct family history of type 2 diabetes, Hispanic ethnicity, age- and sex-specific BMI percentile greater than 85 %, as well as absence of type 1 or type 2 diabetes. Individuals on medications or with a medical condition known to affect glucose or insulin metabolism or body composition were excluded from the study. Current analyses included 312 children with complete measurements of PFAS exposure and protein biomarkers. The USC Institutional Review Board granted ethics approval for this study. Before participation, written informed assent/consent was obtained from participants and their guardians.

2.1.2.   Metabolic and Asthma Incidence Research (Meta-AIR)—To evaluate whether associations in adolescence persist into adulthood, we conducted analyses on 137 young adults aged 17–23 years old from the Meta-AIR cohort, the baseline data of Southern California Children's Health Study (Kim et al., 2019). Inclusion criteria for Meta-AIR were a history of overweight or obesity during high school based on age- and sex-specific BMI percentile greater than the 85th percentile. Individuals were excluded from the study if they were on medications or had a medical condition including type 1 or type 2 diabetes that known to affect glucose or insulin metabolism or body composition. Eligible subjects were contacted and enrolled for a single clinical visit at the Diabetes and Obesity Research or General Clinical Research Center or Clinical Trials Unit at USC between 2014 and 2018. The USC Institutional Review Board granted ethics approval for this study. Before participation, written informed assent/consent was obtained from participants and their guardians if participants were under 18.

2.2.   Data measurement

2.2.1.   Plasma PFAS—PFAS concentrations were measured in plasma samples in batches of 70 study samples by liquid chromatography with high-resolution mass spectrometry (LC-HRMS). Details of the measurement were described elsewhere (Goodrich et al., 2022; Goodrich et al., 2023). PFAS were quantified by dividing the analyte peak with its corresponding internal standard and comparing this ratio to a six-point calibration curve generated utilizing charcoal-stripped plasma. Each batch of 70 samples conducted replicate analyses of the National Institute of Standards and Technology (NIST) 1957 and NIST 1958 standard reference material and included method and instrumental blanks. PFAS had over 90 % of the analyte recovery with less than 15 % of the coefficient of variation. Method accuracy was assessed by comparing with NIST standard reference materials and participating in the Center de toxicologie du Québec's Arctic Monitoring and Assessment Program Ring Test for Persistent Organic Pollutants in Human Serum. Five PFAS congeners commonly reported to have harmful effects in previous literature were included: PFOS, PFOA, PFHS, perfluoroheptanesulfonic acid (PFHpS), and PFNA. The limits of detection (LODs) were 0.43 μg/L for PFOS, 0.01 μg/L for PFHxS, 0.05 μg/L for PFHpS, 0.01 μg/L for PFOA, and 0.01 μg/L for PFNA. All included subjects in the present study had plasma PFAS concentrations that were detectable above the LOD at 100 % of analyzed samples.

2.2.2.   Plasma proteomics—Utilizing the proximity extension assay and a high throughput technique, 369 unique proteins in Olink Explore 384 Cardiometabolic Panel I (https://www.olink.com/content/uploads/2021/08/olink-explore-384-cardiometabolic-protein-list-1.xlsx) were measured in plasma for all included participants. The Olink Explore Cardiometabolic panel was selected for its broader range of cardiometabolic-relevant proteins, facilitating the identification of new associations or a broader exploration of potential biomarkers. Proteins with over 50 % of the observations below LOD were removed ($n = 28$ for SOLAR; $n = 23$ for Meta-AIR), resulting in a total of 341 proteins in SOLAR and 346 proteins in Meta-AIR. The overlapped proteins between SOLAR and Meta-AIR ($n = 334$) were included in statistical analyses. Data values for measurements below the LOD were reported for all samples by Olink. Thus, actual data were used for those falling below LOD to increase the statistical power and achieve a

more normal distribution of the data. Sample controls (pooled plasma samples) were used to assess potential variation between runs and plates. For SOLAR, the average intra-assay and inter-assay coefficient of variance was 12 % and 20 %, respectively. For Meta-AIR, the average intra-assay and inter-assay coefficient of variance was 14 % and 15 %, respectively. Data is presented as Normalized Protein eXpression values, which represent Olink's relative protein quantification units on the log2 scale.

2.2.3. Covariates—Questionnaires were used to collect health history, familial health history, and sociodemographic characteristics from the participants and their guardians. In the SOLAR cohort, socioeconomic status (SES) was assessed using a modified version of the Hollingshead Four-Factor Index (Alderete et al., 2017; Hollingshead, 2011). This index incorporates education, occupation, and marital status of each parent/guardian to provide a single measure for children's social status, with a higher index indicating a higher SES status. The SES index was classified according to the quantiles. There were 35 missing data for SES and thus these children's SES was coded as 'Missing'. As assessed using chi-square tests and independent *t*-tests by previous studies (Goodrich et al., 2021; Goodrich et al., 2023), these children with missing SES data did not have different metabolic or physical attributes including sex, age, or BMI, compared to those with complete SES data. The SES index was analyzed as a categorical variable in the covariate adjustment. Children underwent a physical examination performed by a physician to determine Tanner stage (Marshall and Tanner, 1969,1970). Tanner stage is a scale of development based on secondary sex characteristics, where stage 1 is pre-puberty, stages 2–4 are puberty, and stage 5 is post-puberty. In SOLAR, covariates including age, sex, SES, and study waves were adjusted in Model 1. Tanner stage was further included in Model 2 to improve precision as puberty is an important predictor of cardiometabolic risk in children and adolescents (Low et al., 2022; Moran et al., 1999; Tobisch et al., 2015). In the Meta-AIR cohort, SES was assessed using parental education (Kim et al., 2019). In Meta-AIR, covariates including age, sex, ethnicity (Hispanic/non-Hispanic), and parental education were included in models. Covariates for SOLAR and Meta-AIR were selected based on information obtained from the existing literature and using directed acyclic graphs (DAGs; Figure S1).

2.3. Data analyses

2.3.1. Descriptive statistical analysis—PFAS plasma concentrations were natural logarithm-transformed to limit the influence of extreme values. To examine differences in PFAS levels and study characteristics across two cohorts, we conducted independent *t*-tests on PFAS and continuous covariates, and chi-square tests on the categorical covariates. Spearman correlation analyses were conducted to evaluate the correlation among PFAS levels and among protein concentrations within each cohort. All statistical analyses were performed using R software version 4.1.0.

2.3.2. Protein association study—To examine associations of individual PFAS and PFAS mixtures with each protein, a protein association study was conducted using linear regression through the *"epiomics"* R package. This package is specifically designed for analyzing omics data in observational studies. For individual PFAS, the *"owas"* function was used to examine the associations between individual PFAS and each protein, adjusting for

covariates. Furthermore, we applied the *"owas_qgcomp"* function, using the default setting of a linear effect across quantiles of the mixture, to analyze the associations between tertiles of PFAS mixtures and each protein using quantile g-computation (QGComp; Keil et al., 2020). QGComp is a novel analytical approach used in environmental mixture analysis to estimate the impact of simultaneously increasing all exposures by one quantile. This method allows for the estimation of both the exposure mixture effect and individual contributions to that mixture, without the need for assuming directional homogeneity, linearity, and additivity like weighted quantile sum (WQS) regression (Keil et al., 2020).

Multiple comparisons were adjusted by using a principal component analysis (PCA)-based method to calculate the effective number of tests (M_{eff}) (Wen and Lu, 2011). In brief, PCA was performed on all exposures and all outcomes independently in each cohort to calculate the eigenvalues. The effective number of tests was determined by summing all eigenvalues greater than one for the exposures and for the outcomes using the Kaiser-Guttman rule (Goretzko and Bühner, 2022). The new α level for significance was adjusted by dividing 0.05 over M_{eff} (SOLAR: $M_{eff} = 39$; Meta-AIR: $M_{eff} = 28$). The adjusted significance threshold was 0.05/39 = 0.00128 for SOLAR, and 0.05/28 = 0.00178 for Meta-AIR.

For exploratory analysis, PFAS-protein associations with a two-sided *p*-value < 0.05 were retrieved and further evaluated. To assess the patterns of associations between individual PFAS and significant proteins, heatmaps were generated with k-means clustering on the *t*-statistics in each cohort (Gu, 2022). The optimal number of clusters was determined using gap statistics method (Tibshirani et al., 2002). Labels including "positive associations", "moderate positive associations", and "negative associations" were used to describe the overall pattern of associations between PFAS and proteins, representing their overall direction of association for each cluster.

2.3.3.   Protein-protein interaction network analysis—The protein–protein interaction (PPI) of PFAS-associated proteins with *p* < 0.05 in each cohort was established by the STRING database (version 11.5), a web-based search tool for retrieving interacting genes/proteins (https://string-db.org/). The STRING database provides seven independent 'channels' that categorize association evidence, including three prediction channels based on genomic information, and one channel each for co-expression, text-mining, biochemical/genetic data ('experiments'), and previously curated pathway and protein-complex knowledge ('databases') (Szklarczyk et al., 2018). To ensure the specificity of our analysis, we excluded text-mining evidence as it only considers the co-mention of genes/proteins names in literature without considering the actual reported protein interaction. Each PPI is annotated with one or more scores between one to zero to indicate the confidence level of an interaction. By default, the confidence level thresholds are set at 0.15 for low confidence, 0.40 for medium confidence, 0.70 for high confidence, and 0.90 for highest confidence. The highest interaction score across all other channels (except for the text-mining channel) was considered representative of the strength of the protein interaction. We constructed and visualized the PPI network using Cystoscope software version 3.9.1, by selecting proteins with an interaction score of no less than 0.4 (median confidence level). The specific interaction score was indicated in the figure through the edge type and thickness, with dashed lines for medium confidence (0.4–0.7), solid lines for high

confidence (0.7–0.9), and parallel lines for highest confidence (0.9–1.0). Additionally, we included those proteins that were within a local network cluster identified by STRING to enhance the relevance of our PPI network.

2.3.4.   Pathway analysis—To explore the alterations of biological processes and pathways, Core Analyses (i.e., Functional Analyses) were conducted in the Qiagen Ingenuity Pathway Analysis (IPA) software to analyze identified protein profiling data (Pan et al., 2022). The dataset comprising PFAS-associated proteins, along with their corresponding UniProt IDs and t-statistics obtained from the protein association study, was uploaded into the Qiagen IPA software. The overrepresentation test utilized a customized reference set generated from our input dataset. By utilizing comparison analysis, we examined the Core Analysis results including canonical pathways as well as diseases and functions across various PFAS exposures. Canonical pathways are well-characterized metabolic and cell signaling pathways that have been curated by scientists from Qiagen or third parties. Diseases and functions section provides biological information and diseases related to our results. We first filtered for significant proteins with adjustment for multiple comparisons. Exploratory analysis was further conducted using PFAS-associated proteins with a $p < 0.05$. Pathways and functions with a significant activation z-score ($|z|$ 2) and a Fisher's exact $p < 0.05$ were selected. The derived z-score allows for the inference of activation states, indicating whether the implicated biological processes are "increased" or "decreased". Only pathways and functions involving multiple proteins were presented.

2.3.5.   Cross-database protein annotation—We conducted the annotation of biological functions for the significant proteins identified through adjusting for multiple comparisons, as well as for the proteins with $p < 0.05$ shared between two cohorts. This involved cross-referencing multiple databases, including UniProt, RefSeq, KEGG pathway, and Reactome pathway.

3.   Results

3.1.   Characteristics of the study population

Characteristics of participants and plasma PFAS concentrations in SOLAR and Meta-AIR cohorts are presented in Tables 1 and 2, respectively. The SOLAR cohort recruited between 2001 and 2012, consisted of Hispanic children with a mean (standard deviation, SD) age of 11.3 (1.7) years. The Meta-AIR cohort, recruited between 2014 and 2018, was composed of young adults, 58 % of whom were Hispanic, with a mean (SD) age of 19.9 (1.3) years. The sex distribution was comparable between the two cohorts. In both cohorts, all five PFAS were detected in all participants. Spearman correlation coefficients for PFAS concentrations ranged from 0.01 to 0.93 in SOLAR and from 0.24 to 0.93 in Meta-AIR (Figure S2). PFAS concentrations were consistent with the reported levels observed in the relevant time period and among comparable age groups in NHANES (Centers for Disease Control Prevention, 2019) (Table 2). Spearman correlation coefficients for proteins ranged from −0.57 to 0.96 with a median (interquartile range) of 0.14 (0.20) in SOLAR (Figure S3) and from −0.60 to 0.98 with a median (interquartile range) of 0.17 (0.21) in Meta-AIR (Figure S4).

3.2. PFAS and proteins in SOLAR children cohort

3.2.1. Multiple testing corrections: PFAS exposure was associated with altered protein signatures and functions in SOLAR—Table 3 presents significant PFAS-protein associations after adjusting for multiple comparisons in SOLAR as well as cross-database protein functional annotations. Detailed functional annotations are presented in Table S3. In Model 1, a total of 13 proteins showed significant positive associations with PFAS exposure. Specifically, three proteins were linked to PFOS, three to PFOA, one to PFHpS, seven to PFNA, and one to PFAS mixtures. There was no significant association observed for PFHxS. Only heme oxygenase 1 (HMOX1) and scavenger receptor cysteine rich family member with 5 domains (SSC5D) showed associations with more than one PFAS exposure. HMOX1, an anti-oxidase involved in heme catabolism, was positively associated with PFOA and PFNA. SSC5D, involved in innate defense, was positively associated with PFNA and PFAS Mixtures. Both PFOA and PFNA were positively associated with proteins involved in inflammatory, immune, and antioxidative response, as well as bone metabolism. Specifically, PFOA showed positive associations with c-type lectin domain containing 5A (CLEC5A), eosinophil cationic protein (RNASE3), and HMOX1. CLEC5A regulates osteoclastogenic, inflammation, and immune response, while RNASE3 exhibits antibacterial activity and is related to asthma. In addition, PFNA demonstrated positive associations with acid phosphatase 5 tartrate resistant (ACP5), c-type lectin domain family 1 member A (CLEC1A), HMOX1, and SSC5D. ACP5 is involved in osteoclast differentiation and related to rheumatoid arthritis, while CLEC1A regulates dendritic cell function and is involved in inflammation. In Model 2, additional adjustments were made for tanner stage to enhance the precision of the estimates. Estimates from Model 2 were comparable to those from Model 1, with less than an 11 % change.

Using significant proteins adjusting for multiple comparisons in IPA, we did not identify any pathway or function with a predicted activation z-score. However, diseases and biological functions related to inflammation and respiratory system, as well as cardiovascular disease were shown significant for PFOS (data not shown). For PFOA, all three proteins (i.e., CLEC5A, RNASE3, and HMOX) were involved in inflammation of respiratory system component (Fisher's exact p-value = 0.005, Benjamini-Hochberg (B-H) adjusted p-value = 0.040). RNASE3 and HMOX1 were furthered involved in cell death of cardiomyocytes (Fisher's exact p-value = 0.010, B-H adjusted p-value = 0.042). For PFOS, clusterin-like protein 1 (CLUL1) and neural cell adhesion molecule 1 (NCAM1) were involved in diseases related to endocrine system disorders, including extrapulmonary small cell carcinoma (Fisher's exact p-value < 0.001, B-H adjusted p-value = 0.028) and abdominal neuroendocrine tumor (Fisher's exact p-value = 0.011, B-H adjusted p-value = 0.038).

3.2.2. Exploratory analysis: PFAS was associated with altered proteins signatures, biological processes, and pathways in SOLAR—We conducted additional exploratory analyses of PFAS-protein associations, using a significance threshold of 0.05 for the p-value. Figure S5A presents a heatmap using K-means clustering to illustrate the adjusted associations of PFAS exposure with 134 PFAS-associated proteins in the SOLAR cohort. Similar association patterns were observed between PFNA and PFOA, as well as among PFOS, PFHpS, and PFHxS. Among various PFAS exposure, PFNA

showed significant associations with the largest number of proteins ($n = 72$). Through the utilization of cluster analysis and the gap statistics method to ascertain the optimal number of clusters, we identified three distinct protein clusters. Based on the overall pattern of associations within each cluster, we labeled them as follows: "positive associations" ($n = 45$ proteins), "moderately positive association" ($n = 60$ proteins), and "negative association" ($n = 29$ proteins). Within the "positive associations" cluster, we observed a concordant positive association of three individual PFAS with five proteins, specifically SSC5D, endoglin (ENG), CLUL1, RNASE3, and myeloblastin (PRTN3). In the moderately positively associated cluster, PFNA emerged as the primary compound showing significant associations. Within the "negative associations" cluster, PFOS emerged as the key driver of the observed negative associations. A concordant negative association was found between three individual PFAS and receptor-type tyrosine-protein phosphatase F (PTPRF).

IPA comparison analysis revealed associations of PFOA and PFNA with the activation of canonical pathways related to the immune system (Figure S5B). Specifically, activation of neutrophil degranulation (z-score = 2.65, Fisher's exact p-value = 0.02) was enriched with PFOA exposure, involving seven proteins positively associated with PFOA: RNASE3, CLEC5A, oxidized low-density lipoprotein receptor 1 (OLR1), azurocidin (AZU1), myeloid cell nuclear differentiation antigen (MNDA), myeloblastin (PRTN3), and carcinoembryonic antigen-related cell adhesion molecule 8 (CEACAM8). In addition, PFNA exposure was associated with the activation of immunoregulatory interactions between a lymphoid and non-lymphoid cell (z-score = 2.82, Fisher's exact p-value = 0.03), as well as phagosome formation (z-score = 2.82, Fisher's exact p-value = 0.009). The activation of immunoregulatory interactions between a lymphoid and non-lymphoid cell involved eight proteins positively associated with PFNA: intercellular adhesion molecule 5 (ICAM5), low affinity immunoglobulin gamma Fc region receptor III-B (FCGR3B), integrin beta-1 (ITGB1), cadherin-1 (CDH1), leukocyte immunoglobulin-like receptor subfamily B member 5 (LILRB5), neural proliferation differentiation and control protein 1 (NPDC1), ICAM2, and complement receptor type 2 (CR2). Similarly, the activation of phagosome formation involved eight proteins positively associated with PFNA: HMOX1, prosaposin receptor GPR37 (GPR37), CD209 antigen (CD209), monocyte differentiation antigen CD14 (CD14), FCGR3B, ITGB1, T-cell immunoglobulin and mucin domain-containing protein 4 (TIMD4), and CR2. IPA comparison analysis of diseases and biological functions further demonstrated a significant activation of inflammatory response with PFNA exposure, involving 28 PFNA-associated proteins. Specific proteins involved are presented in Figure S6. No pathway or function remained significant after adjusting for multiple comparisons.

The PPI network among PFAS-associated proteins in the SOLAR cohort is presented in Figure S7. Overall, there were six major network cluster modules including immunoregulatory interactions, JAK-STAT signaling pathway, bone morphogenic protein (BMP) signaling pathway, insulin-like growth factor binding protein (IGFBP), protein digestion, and absorption, as well as apoptotic cell clearance. Within the immunoregulatory interactions module, LILRB1 exhibited a high confidence level of interaction score (0.8) with FCGR3B and FCGR2A in the osteoclast differentiation pathway. Six proteins were clustered in the BMP signaling pathway module including growth/differentiation factor 2 (GDF2), ENG, BMP6, transforming growth factor beta receptor type 3 (TGFBR3),

chordin-like protein 2 (CHRDL2), and ACP5, and were all positively associated with PFAS exposure. Within the JAK-STAT signaling pathway module, leptin (LEP) interacted with platelet-derived growth factor receptor alpha (PDGFRA), oncostatin-M–specific receptor subunit beta (OSMR), interleukin-6 receptor subunit alpha (IL6R), and interleukin-2 receptor subunit alpha (IL2RA) with a medium confidence level of interaction score (0.6).

3.3. PFAS and proteins in Meta-AIR young adults cohort

3.3.1. Multiple testing corrections: PFAS exposure was associated with altered protein signatures in Meta-AIR—Table 4 presents significant PFAS-protein associations after adjusting for multiple comparisons in Meta-AIR. Detailed functional annotations are presented in Table S4. A total of six proteins showed significant associations with PFAS exposure. Specifically, one protein was associated with PFOA, two with PFHxS, one with PFNA, and three with PFAS mixtures. No significant association was observed for PFOS and PFHpS. Only amine oxidase copper containing 3 (AOC3) were associated with more than one PFAS exposure. AOC3, a cell adhesion protein with semicarbazide-sensitive (SSAO) monoamine oxidase activity and potential adipogenesis effect, was negatively associated with PFNA and PFAS mixtures. In addition, PFAS mixtures was positively associated with proteins involved in inflammation and injury response, including GDF15 and IL6. GDF15 is a pleiotropic cytokine related to inflammation, acute injury, and oxidative stress. Similarly, IL6 is a cytokine that functions in inflammation, tissue regeneration upon injury, and immunity, which has been implicated in a variety of inflammation-associated diseases. Besides inflammatory response, we observed a positive association between PFHxS and trypsin-2 (PRSS2), a serine protease secreted by the pancreas which is related to pancreatitis.

Using significant proteins adjusting for multiple comparisons in IPA, we did not identify any pathway or function with a predicted activation z-score. However, we identified PFAS mixtures as the only exposure with significant enrichment (data not shown). Specifically, myocardial infarction involving AOC3, GDF15, and IL6 (Fisher's exact p-value = 0.002, B-H adjusted p-value = 0.047), as well as hypertrophy of cardiomyocytes involving GDF15 and IL6 (Fisher's exact p-value = 0.001, B-H adjusted p-value = 0.047) were significantly enriched.

3.3.2. Exploratory analysis: PFAS was associated with altered proteins signatures, biological processes, and pathways in Meta-AIR—Figure S8A presents a heatmap using K-means clustering to illustrate the adjusted associations of PFAS exposure with 75 significant proteins ($p < 0.05$) in the Meta-AIR cohort. Among various PFAS exposure, PFHxS showed significant associations with the largest number of proteins ($n = 42$). Through the utilization of cluster analysis and the gap statistics method to ascertain the optimal number of clusters, we identified two distinct protein clusters. Based on the overall pattern of associations within each cluster, we labeled them as follows: a cluster of positive associations ($n = 64$ proteins) and a cluster of negative associations ($n = 11$ proteins). Within the cluster of positive associations, we observed concordant positive associations of three individual PFAS with six proteins, specifically GDF2, GDF15, PTPRF, ACP5, collagen alpha-1 (COL18A), and carboxypeptidase A1

(CPA1). In addition, we observed concordant positive associations of four individual PFAS with six proteins, including PRSS2, protein canopy homolog 2 (CNPY2), metalloproteinase inhibitor 1 (TIMP1), IGFBP6, chymotrypsin-like elastase family member 3A (CELA3A), and protein FAM3C (FAM3C). In the cluster of negative associations, we observed concordant negative associations of three individual PFAS with AOC3, and four individual PFAS with neurogenic locus notch homolog protein 3 (NOTCH3).

In the IPA comparison analysis of canonical pathways, we observed that PFHxS (*z*-score = 2.24, Fisher's exact *p*-value = 0.04), PFHpS (*z*-score = 2, Fisher's exact *p*-value = 0.01), and PFAS mixtures (*z*-score = 2.45, Fisher's exact *p*-value = 0.005) demonstrated significant enrichment in activating the regulation of IGF transport and uptake by IGFBPs (Figure S8B). This enrichment involved IL6, TIMP1, and IGFBP6 for all three PFAS. Additional proteins involved in activating the regulation of IGF transport and uptake by IGFBPs included procollagen C-endopeptidase enhancer 1 (PROC) and CDH2 for PFHxS, cystatin-C (CST3) for PFHpS, as well as CST3, PROC, and osteopontin (SPP1) for PFAS mixtures. Additionally, PFHxS was associated with the activation of dendritic cell maturation (*z*-score = 2, Fisher's exact *p*-value = 0.02), involving four positively associated proteins: collagen alpha-1 (COL18A1), COL18A1, IL6, leptin receptor (LEPR), and ICAM1. In the analysis of diseases and biological functions, activation of proliferation of vascular cells was enriched for PFAS mixtures (*z*-score = 2.22, Fisher's exact *p*-value = 0.04), while activation of binding of fibroblast cell lines was enriched for PFHxS (*z*-score = 2.2, Fisher's exact *p*-value = 0.006). Specific proteins involved are presented in Figure S9. No pathway or function remained significant after adjusting for multiple comparisons.

The PPI network among significant proteins in the Meta-AIR cohort is presented in Figure S10. Overall, there were six major network cluster modules including immunoregulatory interactions, JAK-STAT signaling pathways, expression of STAT3-upregulated extracellular proteins, digestion and cell wall disruption, collagen formation & matrix metalloproteinases, and blood coagulation. Within the immunoregulatory interactions module, FCGR2A exhibited a high confidence level of interaction score (0.8) with LILRB2 and LILRB5 in the osteoclast differentiation pathway. There were five PFAS positively associated proteins related to digestion including CPA1, CELA3A, PRSS2, ribonuclease T2 (RNASET2), and angiogenin (ANG). Specifically, CPA1, CELA3A, and PRSS2 were associated with pancreatitis. IL6, OSMR, thrombopoietin (THPO), LEPR, and IL19 interacted with a medium confidence level of interaction score (0.6) in the JAK-STAT signaling pathway. Three PFAS positively associated proteins (i.e., TIMP1, LBP, and IL6) interacted with each other with highest confidence level of interaction score (0.9) in the expression of STAT3-upregulated extracellular protein.

3.4. Shared PFAS and protein associations in SOLAR and Meta-Air

We identified an overlap of 30 proteins that exhibited significant associations with at least one PFAS in both cohorts (Fig. 1). Table S1 presents the β (95 % CI) and biological functions of 25 significant proteins showing concordant associations with PFAS. Among these, 24 proteins demonstrated concordant positive associations. These PFAS positively associated proteins are involved in a range of shared biological functions, including: (1)

bone metabolism involving ACP5, SPP1, CLEC5A, GDF2, dickkopf-related protein 3 (DKK3); (2) anti-angiogenesis involving COL18A1, basement membrane-specific heparan sulfate proteoglycan core protein (HSPG2), and GDF2; (3) pro-inflammation involving SPP1, CLEC5A, and galectin-3 (LGALS3); (4) immune responses involving membrane attack complex inhibition factor (CD59), LGALS3, OSMR, ICAM2; (5) neurological functions involving GPR37 and SLIT and NTRK-like protein 6 (SLITRK6).

When comparing the same PFAS-protein association shared between two cohorts, we observed 11 proteins exhibiting significant associations. Specifically, concordant positive associations were identified for the following PFAS-protein pairs: COL18A1, FABP4, and ICAM2 with PFNA; CD59 with PFNA and PFAS mixtures; ACP5, HSPG2, and SPP1 with PFAS mixtures; DKK3 and GDF2 with PFOS; and cadherin-related family member 5 (CDHR5) with PFHpS. FCGR2A with biological functions of phagocytosis and clearing of immune responses exhibited a concordant negative association with PFOS across the two cohorts. Furthermore, we observed that the associations of PFHxS, PFHpS, and PFOA with PTPRF were in opposite directions across the two cohorts, showing negative associations in SOLAR and positive associations in Meta-AIR.

4. Discussion

The application of omics in environmental epidemiology has been emerging as a valuable tool to develop mechanistic insights into potential environmental-associated disease risk. However, epidemiological studies on PFAS and proteomics are scarce. In particular, there is no existing epidemiological study examining proteomic profiles of PFAS mixtures. While single exposure models offer insights into the health effects of individual PFAS compounds, they fail to consider simultaneous exposure to multiple potentially correlated environmental factors in real life, which may result in synergistic effects. To our knowledge, this study is the first to evaluate the associations between PFAS exposure and cardiometabolic relevant proteome in Hispanic adolescents and young adults with high BMI. Our study on PFAS exposure in overweight/obese adolescents with high metabolic risk and at a critical developmental stage marked by metabolic changes, have significance in identifying novel biomarkers reflecting PFAS-associated risk. Our replication in young adults can further evaluate the persistence of such effect from adolescents to adulthood.

Results after adjusting for multiple comparisons revealed that plasma levels of individual PFAS and PFAS mixtures were associated with several proteomic biomarkers related to immune response, inflammation, and oxidative stress in both cohorts. Such findings align with our exploratory analysis results. Specifically, we identified significant activations of immune-related pathways in pathway analysis and the presence of similar network clusters such as JAK-STAT signaling and immunoregulatory network through PPI network analysis in both cohorts. In addition, our exploratory analysis identified shared PFAS and protein associations, featuring 10 proteins with shared positive associations and one protein (i.e. FCG2RA) with shared negative associations. These proteins are involved in pro-inflammation, immune responses, bone metabolism, and anti-angiogenesis. Our novel findings on PFAS-protein associations provide potential molecular evidence of PFAS toxicity.

4.1. Inflammation and JAK-STAT signaling

In SOLAR, results after adjusting for multiple comparisons showed that PFNA demonstrated significant positive associations with the largest number of proteins, including ACP5, CLEC1A, HMOX1, LRP11, MCAM, SPARCL1, and SSC5D. After considering the mixture effect of PFAS, only SSC5D remained significant. SSC5D is a novel soluble protein belong to the scavenger receptor cysteine-rich superfamily, which is associated with innate response and inflammation (Bessa Pereira et al., 2016). A recent study found significant elevated levels of SSC5D in patients and mouse with heart failure, compared with those without heart failure condition (Ge et al., 2023). Although we did not find the exact proteins that were significant in Meta-AIR after adjusting for multiple comparisons, we still observed PFAS alterations of proteins with similar functions. For example, PFAS mixtures showed significant positive associations with two inflammatory proteins (i.e., GDF15 and IL6). This association was significantly enriched with the hypertrophy of cardiomyocytes function in our pathway analysis. Additionally, GDF15 and IL6 have been identified as biomarkers of adverse cardiac events by numerous studies (Rochette et al., 2021; Su et al., 2021). Our findings adjusted for multiple comparisons provide evidence of PFAS-associated pro-inflammation and suggest their potential mediation roles in cardiometabolic conditions in children and young adults.

In line with our findings adjusted for multiple comparison, our exploratory analysis identified a concordant positive association between PFAS mixtures and SPP1, a protein associated with inflammation. Furthermore, we found that PFAS exposure was associated with alterations of proteins involved in the JAK-STAT signaling pathway in both cohorts. The JAK-STAT signaling pathway plays a major role in inflammatory responses, immune cell development, stem cell maintenance, organismal growth, and hematopoiesis (Thomas et al., 2015). Specifically, we observed positive associations of PFNA with IL6R and OSMR in SOLAR. Similar positive associations of PFHxS, PFHpS, and PFAS mixtures with IL6, as well as between PFHxS and OSMR were found in Meta-AIR. In Meta-AIR, we further observed a significant activation of inflammatory response associated with PFNA from IPA. Despite the overall coherence in our findings regarding PFAS-associated pro-inflammation, previous studies have reported some inconsistent results. Our results focusing on Hispanic young populations with a history of overweight or obesity were consistent with a previous longitudinal study of predominantly non-white, low-income, overweight or obese California women during pregnancy and postpartum, which found positive associations of PFAS (i.e., PFOS, PFOA, and PFAS mixtures) and other endocrine-disrupting chemicals (e.g., PBDEs) with IL6 (Zota et al., 2018). However, recent proteomics studies on the Swedish middle-aged (Salihovic et al., 2020) and older-aged populations (Dunder et al., 2023) found negative cross-sectional associations of PFOS and PFDA with proteomic inflammatory biomarkers such as IL6 and GDF15. Such divergent findings might result from differences in study populations and designs. Future work is warranted to investigate potential mechanisms whereby age and health conditions (e.g., BMI) might contribute to modifying PFAS effects on inflammation.

4.2. Immunosuppression

Although the evidence for the immunotoxicity of PFAS corroborates across experimental animal studies (NTP, 2016), findings are inconsistent in epidemiological studies (Chang et al., 2016). For instance, a review revealed strong evidence of reduced antibody response to certain vaccines in the presence of PFOA and PFOS exposure in children, indicating potential immunosuppression (von Holst et al., 2021). However, studies conducted on adults have yielded inconsistent associations with immune outcomes (Antoniou et al., 2022).

In our study, we observed that PFAS exposure was associated with alterations in immunoregulatory proteins. Specifically, we identified positive associations for several human inhibitory leukocyte Ig-like receptors (LILRBs), such as PFNA with LILRB1 in SOLAR, as well as PFHxS, PFOA, and PFAS mixtures with LILRB2, and PFNA with LILRB5 in Meta-AIR. Additionally, negative associations were found of PFOS with FCGR2A in SOLAR, and of PFOS and PFAS mixtures with FCGR2A in Meta-AIR. Previous research has reported that LILRBs contribute to immunosuppression, leading to tolerance or immune-evasion (De Louche and Roghanian, 2022), while FCGR2A initiates cellular responses against pathogens and soluble antigens by binding to IgG (Junker et al., 2020). Our findings of PFAS-associated upregulation of LILRB1, 2, 5 and downregulation of FCGR2A provide potential explanations for the observed immunosuppressive effects of PFAS. These findings are consistent with earlier transcriptomics research in human population. This research demonstrated PFAS-associated immunomodulation, characterized by perturbed adaptive immunity in a cross-sectional study of Czech adults (Rudzanová et al., 2024), as well as impaired immune function in a Norwegian longitudinal birth cohort study (Pennings et al., 2016).

4.3. Immune hypersensitivity

While extensive research has been focusing on the immunosuppressive effects of PFAS, limited epidemiological studies have explored the connection between PFAS and immunoenhancement because of the difficulty of diagnosing hypersensitivities (DeWitt et al., 2019). Specifically, evidence regarding the effects of PFAS exposure on infectious diseases is inconsistent, and there have been limited studies investigating hypersensitivity reactions including type I hypersensitivities (e. g., allergies and asthma) and autoimmune diseases (e.g., ulcerative colitis, rheumatoid arthritis, and lupus) (Antoniou et al., 2022; DeWitt et al., 2019; von Holst et al., 2021). Recent studies on rheumatoid arthritis reported positive associations of PFAS with rheumatoid factors (Qu et al., 2022) and Disease Activity Score 28 (DSA28) (Zhao et al., 2022). A large retrospective cohort study conducted on a population with high PFAS exposure discovered a significant increase in the incidence of ulcerative colitis linked to PFOA exposure (Steenland et al., 2013). These findings suggest that, apart from potential immunosuppression, PFAS may also have hyperstimulation effects on the immune system, leading to an increased risk of autoimmune diseases. However, the specific mechanisms of PFAS immunotoxicity in humans remain largely undefined (Chang et al., 2016).

In SOLAR, using IPA, we identified significant activations of immunoregulatory interactions and phagosome formation associated with PFNA, as well as a significant activation of

neutrophil degranulation associated with PFOA. In Meta-AIR, we identified a significant activation of dendritic cell maturation associated with PFHxS. Neutrophil degranulation, a crucial process in innate immunity, can become problematic when excessively triggered, as observed in numerous immune and inflammatory disorders, including asphyxic episodes of asthma, acute lung injury, rheumatoid arthritis, and septic shock (Lacy, 2006). Dendritic cells and other antigen-presenting cells (APCs) mediate the phagocytosis by extracting antigens from material digested in phagosomes for presentation to lymphocytes, thereby contributing to the activation of T cells and the initiation of adaptive immune responses (Besnard et al., 2011). Similarly, disruptions in dendritic cell homoeostasis have been implicated in various human inflammatory and autoimmune diseases (Blanco et al., 2008). Thus, our findings provide additional evidence at the cellular level, suggesting the potential immunoenhancement toxicity of PFAS in humans through the activation of cellular immune responses.

4.4. Bone metabolism

Previous epidemiological studies found that PFAS exposure was associated with adverse bone outcomes, such as reduced bone mineral density in children (Blomberg et al., 2022; Højsager et al., 2023), adolescents (Beglarian et al., 2024; Carwile et al., 2022), and adults (Khalil et al., 2016), as well as increased osteoporosis in women (Khalil et al., 2016). In our study, we identified concordant positive associations of PFAS exposure with several proteins related to bone metabolism, such as ACP5, SPP1, CLEC5A, DKK3, and GDF2. Specifically, PFAS mixtures was positively associated with ACP5 and SPP1 in both cohorts.

ACP5, also known as tartrate-resistant acid phosphatase (TRAP), is an osteoclastic enzyme involved in bone matrix degradation and serves as a good serum marker for bone resorption (Halleen et al., 2006; Shaw and Högler, 2012). Studies have shown an inverse relationship between levels of TRAPb and bone mineral density in postmenopausal women, as well as a significantly elevated levels of TRAPb in women with osteoporosis compared to controls (Halleen et al., 2002; Mederle et al., 2018). SPP1, a highly phosphorylated sialoprotein mainly produced by osteoblasts, plays a pivotal role in various biological processes, including the endocrine-regulation of bone mass, biomineralization, inflammation, fibrosis, tumorigenesis, and metastasis (Farrokhi et al., 2018). Increased expression of SPP1 has been linked to several bone-related diseases such as osteoporosis, rheumatoid arthritis, and osteosarcoma (Si et al., 2020).

While the biological functions of ACP5 and SPP1 in bone metabolism have been relatively well-studied, the roles of CLEC5A and DKK3 in bone-related processes remain less understood. CLEC5A has been established as a positive regulator of osteoclastogenesis in mouse (Inui et al., 2009). Furthermore, in a mouse experiment, the activation of CLEC5A enhanced the recruitment of inflammatory cytokines to the joints and promoted bone erosion, indicating its role in immune-mediated skeletal disorders (Joyce-Shaikh et al., 2010). The DKK family has been shown to inhibit the Wnt/β-catenin signaling pathway, which is a key regulator of bone remodeling (Dincel and Jørgensen, 2023). Specifically, DKK1, the most extensively studied subtype expressed by mature osteoblasts and osteocytes (Zhang et al., 2004), has been associated with low bone mineral density in adolescent

patients (Wiromrat et al., 2023) and with fresh hip fractures in the elderly in a case-control study (Wanby et al., 2016).

Our findings of the positive associations of PFAS with these proteins produced by bone tissues, including ACP5, SPP1, CLEC5A, and DKK3, provide insights into the potential mechanistic osteotoxicity of PFAS. It is noteworthy that we also observed a positive association between PFOS and an osteogenic protein, GDF2, in both cohorts. GDF2, a pleiotropic cytokine mainly produced by liver (Bidart et al., 2012; Desroches-Castan et al., 2022), is known for being one of the most potent BMPs (i.e., BMP9) that can induce osteoclast differentiation, both in vitro and in vivo (Luu et al., 2007; Tang et al., 2009). While the osteogenic function of GDF2 may seem contradictory to prior epidemiological findings regarding the adverse effects of PFAS on bone health, it's important to understand that GDF2 has a broad range of biological functions. These functions include anti-angiogenesis (David et al., 2008), involvement in hepatic fibrosis and regeneration, and tumorigenesis (Mostafa et al., 2019). Notably, recent animal experimental work by the Breitkopf-Heinlein team has found that GDF2 is primarily produced by hepatic stellate cells and plays a pro-fibrogenic and pro-inflammatory role upon tissue damage (Jiang et al., 2021). Elevated levels of GDF2 have been shown to enhance liver damage and fibrogenesis during injuries (Breitkopf-Heinlein et al., 2017). Our finding on PFAS-associated upregulation of the pro-inflammatory and pro-fibrogenic protein GDF2, aligns with one of our findings of the positive associations of PFAS with several pro-inflammatory proteins, including GDF15 and IL6. These proteins play crucial roles in stress response following injury and tissue regeneration.

4.5. Other findings

Besides the above overlapping findings, we identified unique findings in Meta-AIR from IPA, such as the activation of regulation of IGF transport and uptake by IGFBPs associated with PFHxS, PFHpS, and PFAS mixtures, as well as the activation of proliferation of vascular cells associated with PFAS mixtures. Previous studies revealed that excessive proliferation of vascular smooth muscle cells contributes to the development of various diseases, such as atherosclerosis, restenosis, and pulmonary hypertension (Wang et al., 2018). Although the pathogenesis of the activation of regulation related to IGF and IGBPs remains unknown, IGF plays key a role in cardiac development (Díaz Del Moral et al., 2021). Consequently, the proteins involved in these pathways may serve as potential mediators of associations between PFAS and cardiometabolic outcomes. Further primary research is needed to fully understand these relationships.

Our study did find certain inconsistent associations. Specifically, we observed that the associations of PFHxS, PFHpS, and PFOA with PTPRF were in opposite directions across the two cohorts, showing negative associations in SOLAR and positive associations in Meta-AIR. PTPRF has been shown to modulate beta-catenin signaling (Aicher et al., 1997) and is implicated in insulin signaling and secretion (Sevillano et al., 2021). An increased expression of PTPRF has been found in the pathogenesis of insulin resistance in some animal experiments (Krüger et al., 2015; Kulas et al., 1995; Zabolotny et al., 2001) and a human case-control study (Ahmad et al., 1995; Sevillano et al., 2021).

Therefore, our findings of negative associations in SOLAR and positive associations in Meta-AIR imply a PFAS-associated insulin resistance, as indicated by PTPRF, decreasing in children, and increasing in young adults. These results suggest that the PFAS association with cardiometabolic outcomes, as supported by existing literature, may involve distinct biological mechanisms and mediation pathways in children compared to adults. However, it is crucial to note that our findings, indicating opposite directions of associations, were not adjusted for multiple comparisons. Hence, caution is warranted in drawing conclusions.

5. Strengths and limitations

This is the first study examining PFAS associations with alterations in high-throughput proteomic profiles relevant to cardiometabolism among Hispanic adolescents and young adults, contributing valuable insights into the potential PFAS mechanistic toxicity at the molecular level. Our study adjusted for confounders according to the characteristics of the study population, which minimized potential confounding bias and enhanced the internal validity of our results. More importantly, we incorporated QGComp to evaluate the PFAS mixtures effect, addressing a gap in the existing literature concerning the proteomic profiles of co-exposure to correlated PFAS. It is important to note, however, that our study only considered five PFAS congeners, while humans may also experience co-exposure to other potentially correlated environmental pollutants. Future exposome research incorporating a broader range of environmental exposures would be advantageous for a more comprehensive evaluation of the mixture effects on human health. Proteomic analysis in epidemiological studies can be influenced by within/between-person variability, posing challenges to stability and reproducibility. However, our utilization of Olink, employing a novel high-throughput proximity extension assay technology, has been validated for technical robustness with good reproducibility and stability in numerous studies (Carlyle et al., 2022; Haslam et al., 2022). Additionally, our quality control results, indicating acceptable coefficients of variation, provide further support for the reliability of our results. While our study fills a critical gap in epidemiological research on PFAS and proteomics, our focus on targeted proteomics may limit biomarker discovery. The incorporation of untargeted proteomics in future investigations will be beneficial to further evaluate PFAS-associated risk. Our focus on individuals at high metabolic risk can be useful for targeted disease prevention. However, the findings may not be easily generalized to the general health population. Lastly, the cross-sectional study design restricts our ability to establish a causal relationship between PFAS and the observed alterations in proteomic profiles. However, the persistent nature of PFAS exposure, characterized by long biological half-lives (Li et al., 2018; Nicole, 2020), mitigates the risk of reverse causality, as it reflects historical exposure profiles.

5.1. Future implications

Our findings offer novel insights into the protein profiles associated with PFAS exposure in young populations, contributing to a deeper understanding of the effects of PFAS in humans. Several biological processes and pathways that are highlighted in our study, including immune-related pathways, inflammatory response, JAK-STAT signaling, and bone metabolism, play important roles in various health conditions. Future studies can focus on investigating the role of specific proteins involved in these biological processes and

pathways, thereby elucidating their mediation effect between PFAS and the development of various diseases, including cardiometabolic conditions, immune-related disorders, cancer, and bone-related health conditions.

6. Conclusions

Our study is one of the first to evaluate the associations of PFAS exposure with cardiometabolic proteomics in Hispanic young populations. Plasma levels of PFAS were associated with broad alterations of the proteomic profiles specifically linked to disrupted immune-related functions and JAK-STAT signaling. The overlapping proteins in both cohorts associated with PFAS exposure additionally shared similar functions related to pro-inflammation, immune responses, bone metabolism, and anti-angiogenesis. Our findings provide crucial molecular-level evidence of PFAS effects in humans and propose potential biological mechanistic insights linking PFAS exposure to human diseases.

Supplementary Material

Refer to Web version on PubMed Central for supplementary material.

Acknowledgements

Data availability

Data will be made available on request.

References

Ahmad F, Considine RV, Goldstein BJ, 1995. Increased abundance of the receptor-type protein-tyrosine phosphatase lar accounts for the elevated insulin receptor dephosphorylating activity in adipose tissue of obese human subjects. J. Clin. Invest 95, 2806–2812. [PubMed: 7769120]

Aicher B, Lerch MM, Müller T, Schilling J, Ullrich A, 1997. Cellular redistribution of protein tyrosine phosphatases lar and ptpσ by inducible proteolytic processing. J. Cell Biol 138, 681–696. [PubMed: 9245795]

Alderete TL, Habre R, Toledo-Corral CM, Berhane K, Chen Z, Lurmann FW, et al. , 2017. Longitudinal associations between ambient air pollution with insulin sensitivity, β-cell function, and adiposity in los angeles latino children. Diabetes 66, 1789–1796. [PubMed: 28137791]

Antoniou E, Colnot T, Zeegers M, Dekant W, 2022. Immunomodulation and exposure to per- and polyfluoroalkyl substances: an overview of the current evidence from animal and human studies. Arch. Toxicol 96, 2261–2285. [PubMed: 35695909]

Attema B, Janssen AWF, Rijkers D, van Schothorst EM, Hooiveld G, Kersten S, 2022. Exposure to low-dose perfluorooctanoic acid promotes hepatic steatosis and disrupts the hepatic transcriptome in mice. Molecular Metabolism 66, 101602. [PubMed: 36115532]

Beglarian E, Costello E, Walker DI, Wang H, Alderete TL, Chen Z, et al. , 2024. Exposure to perfluoroalkyl substances and longitudinal changes in bone mineral density in adolescents and young adults: a multi-cohort study. Environ. Res 244, 117611. [PubMed: 38061983]

Besnard A-G, Togbe D, Guillou N, Erard F, Quesniaux V, Ryffel B, 2011. Il-33-Activated Dendritic Cells Are Critical for Allergic Airway Inflammation. 41, 1675–1686.

Bessa Pereira C, Bocková M, Santos RF, Santos AM, Martins de Araújo M, Oliveira L, et al. , 2016. The scavenger receptor ssc5d physically interacts with bacteria through the srcr-containing n-terminal domain. Front. Immunol 7, 416. [PubMed: 27790215]

Bidart M, Ricard N, Levet S, Samson M, Mallet C, David L, et al. , 2012. Bmp9 is produced by hepatocytes and circulates mainly in an active mature form complexed to its prodomain. Cell. Mol. Life Sci 69, 313–324. [PubMed: 21710321]

Blanco P, Palucka AK, Pascual V, Banchereau J, 2008. Dendritic cells and cytokines in human inflammatory and autoimmune diseases. Cytokine Growth Factor Rev. 19, 41–52. [PubMed: 18258476]

Blomberg A, Mortensen J, Weihe P, Grandjean P, 2022. Bone mass density following developmental exposures to perfluoroalkyl substances (pfas): a longitudinal cohort study. Environmental Health : a Global Access Science Source 21, 113. [PubMed: 36402982]

Breitkopf-Heinlein K, Meyer C, König C, Gaitantzi H, Addante A, Thomas M, et al. , 2017. Bmp-9 interferes with liver regeneration and promotes liver fibrosis. Gut 66, 939–954. [PubMed: 28336518]

Calafat AM, Kato K, Hubbard K, Jia T, Botelho JC, Wong LY, 2019. Legacy and alternative per- and polyfluoroalkyl substances in the u.s. general population: paired serum-urine data from the 2013–2014 national health and nutrition examination survey. Environ Int 131, 105048.

Carlyle BC, Kitchen RR, Mattingly Z, Celia AM, Trombetta BA, Das S, et al. , 2022. Technical performance evaluation of olink proximity extension assay for blood-based biomarker discovery in longitudinal studies of alzheimer's disease. Front. Neurol 13, 889647.

Carwile JL, Seshasayee SM, Ahrens KA, Hauser R, Driban JB, Rosen CJ, et al. , 2022. Serum pfas and urinary phthalate biomarker concentrations and bone mineral density in 12–19 year olds: 2011–2016 nhanes. J. Clin. Endocrinol. Metab 107, e3343–e3352. [PubMed: 35511700]

Casazza K, Goran MI, Gower BA, 2008. Associations among insulin, estrogen, and fat mass gain over the pubertal transition in african-american and european-american girls. J. Clin. Endocrinol. Metab 93, 2610–2615. [PubMed: 18349063]

Centers for Disease Control Prevention. 2019. Fourth report on human exposure to environmental chemicals, updated tables.

Chang ET, Adami HO, Boffetta P, Wedner HJ, Mandel JS, 2016. A critical review of perfluorooctanoate and perfluorooctanesulfonate exposure and immunological health conditions in humans. Crit. Rev. Toxicol 46, 279–331. [PubMed: 26761418]

Chung ST, Onuzuruike AU, Magge SN, 2018. Cardiometabolic risk in obese children. Ann. N. Y. Acad. Sci 1411, 166–183. [PubMed: 29377201]

Costello E, Rock S, Stratakis N, Eckel SP, Walker DI, Valvi D, et al. , 2022. Exposure to per- and polyfluoroalkyl substances and markers of liver injury: a systematic review and meta-analysis. Environ. Health Perspect 130, 46001. [PubMed: 35475652]

Cousins IT, Ng CA, Wang Z, Scheringer M, 2019. Why is high persistence alone a major cause of concern? Environ. Sci. Processes Impacts 21, 781–792.

David L, Mallet C, Keramidas M, Lamandé N, Gasc JM, Dupuis-Girod S, et al. , 2008. Bone morphogenetic protein-9 is a circulating vascular quiescence factor. Circ. Res 102, 914–922. [PubMed: 18309101]

De Louche CD, Roghanian A. 2022. Human inhibitory leukocyte ig-like receptors: From immunotolerance to immunotherapy. JCI insight 7.

Desroches-Castan A, Tillet E, Bouvard C, Bailly S, 2022. Bmp9 and bmp10: two close vascular quiescence partners that stand out. Developmental Dynamics : an Official Publication of the American Association of Anatomists 251, 178–197. [PubMed: 34240497]

DeWitt JC, Blossom SJ, Schaider LA, 2019. Exposure to per-fluoroalkyl and polyfluoroalkyl substances leads to immunotoxicity: epidemiological and toxicological evidence. J. Eposure Sci. Environ. Epidemiol 29, 148–156.

Díaz Del Moral S, Benaouicha M, Muñoz-Chápuli R, Carmona R. 2021. The insulin-like growth factor signalling pathway in cardiac development and regeneration. International journal of molecular sciences 23.

Dincel AS, Jørgensen NR, 2023. New emerging biomarkers for bone disease: sclerostin and dickkopf-1 (dkk1). Calcif. Tissue Int 112, 243–257. [PubMed: 36165920]

Dubois-Deruy E, Peugnet V, Turkieh A, Pinet F, 2020. Oxidative Stress in Cardiovascular Diseases. 9, 864.

Dunder L, Salihovic S, Lind PM, Elmstahl S, Lind L, 2023. Plasma levels of per- and polyfluoroalkyl substances (pfas) are associated with altered levels of proteins previously linked to inflammation, metabolism and cardiovascular disease. Environ Int 177, 107979.

Ehrlich V, Bil W, Vandebriel R, Granum B, Luijten M, Lindeman B, et al. , 2023. Consideration of pathways for immunotoxicity of per- and polyfluoroalkyl substances (pfas). Environ. Health 22, 19. [PubMed: 36814257]

Evans N, Conley JM, Cardon M, Hartig P, Medlock-Kakaley E, Gray LE Jr., 2022. In vitro activity of a panel of per- and polyfluoroalkyl substances (pfas), fatty acids, and pharmaceuticals in peroxisome proliferator-activated receptor (ppar) alpha, ppar gamma, and estrogen receptor assays. Toxicol. Appl. Pharmacol 449, 116136. [PubMed: 35752307]

Farrokhi V, Chabot JR, Neubert H, Yang Z, 2018. Assessing the feasibility of neutralizing osteopontin with various therapeutic antibody modalities. Sci. Rep 8, 7781. [PubMed: 29773891]

Fiordelisi A, Iaccarino G, Morisco C, Coscioni E, Sorriento D, 2019. Nfkappab is a key player in the crosstalk between inflammation and cardiovascular diseases. Int. J. Mol. Sci 20.

Ge Y, Liu X, Chen H, Li G, Xing X, Liu J, et al. , 2023. The serum soluble scavenger with 5 domains levels: a novel biomarker for individuals with heart failure. Front. Physiol 14, 1140856.

Ghigo A, Laffargue M, Li M, Hirsch E, 2017. Pi3k and Calcium Signaling in Cardiovascular Disease. 121, 282–292.

Goodrich JA, Alderete TL, Baumert BO, Berhane K, Chen Z, Gilliland FD, et al., 2021. Exposure to Perfluoroalkyl Substances and Glucose Homeostasis in Youth. 129, 097002.

Goodrich JA, Walker D, Lin X, Wang H, Lim T, McConnell R, et al. , 2022. Exposure to perfluoroalkyl substances and risk of hepatocellular carcinoma in a multiethnic cohort. JHEP Reports 4, 100550.

Goodrich JA, Walker DI, He J, Lin X, Baumert BO, Hu X, et al., 2023. Metabolic Signatures of Youth Exposure to Mixtures of per- and Polyfluoroalkyl Substances: A Multi-Cohort Study. 131, 027005.

Goretzko D, Bühner M, 2022. Factor retention using machine learning with ordinal data. Appl. Psychol. Meas 46, 406–421. [PubMed: 35812814]

Gu Z, 2022. Complex Heatmap Visualization. 1, e43.

Gui SY, Qiao JC, Xu KX, Li ZL, Chen YN, Wu KJ, et al. , 2023. Association between per- and polyfluoroalkyl substances exposure and risk of diabetes: a systematic review and meta-analysis. J Expo Sci Environ Epidemiol 33, 40–55. [PubMed: 35970987]

Guo H, Wang L, Deng Y, Ye J, 2021. Novel perspectives of environmental proteomics. Sci. Total Environ 788, 147588.

Halleen JM, Ylipahkala H, Alatalo SL, Janckila AJ, Heikkinen JE, Suominen H, et al. , 2002. Serum tartrate-resistant acid phosphatase 5b, but not 5a, correlates with other markers of bone turnover and bone mineral density. Calcif. Tissue Int 71, 20–25. [PubMed: 12073156]

Halleen JM, Tiitinen SL, Ylipahkala H, Fagerlund KM, Väänänen HK, 2006. Tartrate-resistant acid phosphatase 5b (tracp 5b) as a marker of bone resorption. Clin. Lab 52, 499–509. [PubMed: 17078477]

Haslam DE, Li J, Dillon ST, Gu X, Cao Y, Zeleznik OA, et al. , 2022. Stability and Reproducibility of Proteomic Profiles in Epidemiological Studies: Comparing the Olink and Somascan Platforms. 22, 2100170.

Højsager FD, Sigvaldsen A, Andersen MS, Juul A, Nielsen F, Möller S, et al. , 2023. Prenatal and early postnatal exposure to perfluoroalkyl substances and bone mineral content and density in the odense child cohort. Environ Int 181, 108264.

Hollingshead AB, 2011. Four factor index of social status. Yale Journal of Sociology 8, 21–51.

Inui M, Kikuchi Y, Aoki N, Endo S, Maeda T, Sugahara-Tobinai A, et al. 2009. Signal adaptor dap10 associates with mdl-1 and triggers osteoclastogenesis in cooperation with dap12. Proceedings of the National Academy of Sciences of the United States of America 106:4816–4821. [PubMed: 19251634]

Jiang Q, Li Q, Liu B, Li G, Riedemann G, Gaitantzi H, et al. , 2021. Bmp9 promotes methionine- and choline-deficient diet-induced nonalcoholic steatohepatitis in non-obese mice by enhancing nf-κb dependent macrophage polarization. Int. Immunopharmacol 96, 107591. [PubMed: 33812253]

Joyce-Shaikh B, Bigler ME, Chao CC, Murphy EE, Blumenschein WM, Adamopoulos IE, et al. , 2010. Myeloid dap12-associating lectin (mdl)-1 regulates synovial inflammation and bone erosion associated with autoimmune arthritis. J. Exp. Med 207, 579–589. [PubMed: 20212065]

Junker F, Gordon J, Qureshi O, 2020. Fc gamma receptors and their role in antigen uptake, presentation, and t cell activation. Front. Immunol 11, 1393. [PubMed: 32719679]

Karhunen V, Gill D, Huang J, Bouras E, Malik R, Ponsford MJ, et al. , 2023. The interplay between inflammatory cytokines and cardiometabolic disease: bi-directional mendelian randomisation study. BMJ Medicine 2, e000157.

Keil AP, Buckley JP, O'Brien KM, Ferguson KK, Zhao S, White AJ, 2020. A Quantile-Based g-Computation Approach to Addressing the Effects of Exposure Mixtures. 128, 047004.

Kelly LA, Lane CJ, Weigensberg MJ, Toledo-Corral CM, Goran MI, 2011. Pubertal changes of insulin sensitivity, acute insulin response, and β-cell function in overweight latino youth. J. Pediatr 158, 442–446. [PubMed: 20888012]

Khalil N, Chen A, Lee M, Czerwinski SA, Ebert JR, DeWitt JC, et al. , 2016. Association of perfluoroalkyl substances, bone mineral density, and osteoporosis in the u.s. population in nhanes 2009–2010. Environ. Health Perspect 124, 81–87. [PubMed: 26058082]

Kim JS, Chen Z, Alderete TL, Toledo-Corral C, Lurmann F, Berhane K, et al. , 2019. Associations of air pollution, obesity and cardiometabolic health in young adults: the meta-air study. Environ. Int 133, 105180.

Kirk AB, Michelsen-Correa S, Rosen C, Martin CF, Blumberg B, 2021. Pfas and potential adverse effects on bone and adipose tissue through interactions with pparγ. Endocrinology 162.

Kissa E. 2001. Fluorinated surfactants and repellents:CRC Press.

Krüger J, Brachs S, Trappiel M, Kintscher U, Meyborg H, Wellnhofer E, et al. , 2015. Enhanced insulin signaling in density-enhanced phosphatase-1 (dep-1) knockout mice. Molecular Metabolism 4, 325–336. [PubMed: 25830095]

Kulas DT, Zhang WR, Goldstein BJ, Furlanetto RW, Mooney RA, 1995. Insulin receptor signaling is augmented by antisense inhibition of the protein tyrosine phosphatase lar. J. Biol. Chem 270, 2435–2438. [PubMed: 7852302]

Kyrtopoulos SA, 2013. Making Sense of Omics Data in Population-Based Environmental Health Studies. 54, 468–479.

Lacy P, 2006. Mechanisms of degranulation in neutrophils. Allergy, Asthma, and Clinical Immunology : Official Journal of the Canadian Society of Allergy and Clinical Immunology 2, 98–108. [PubMed: 20525154]

Lewis RC, Johns LE, Meeker JD, 2015. Serum biomarkers of exposure to perfluoroalkyl substances in relation to serum testosterone and measures of thyroid function among adults and adolescents from nhanes 2011–2012. Int. J. Environ. Res. Public Health 12, 6098–6114. [PubMed: 26035660]

Li Y, Fletcher T, Mucs D, Scott K, Lindh CH, Tallving P, et al. , 2018. Half-lives of pfos, pfhxs and pfoa after end of exposure to contaminated drinking water. Occup Environ Med 75, 46–51. [PubMed: 29133598]

Liu B, Zhu L, Wang M, Sun Q, 2023. Associations between per- and polyfluoroalkyl substances exposures and blood lipid levels among adults-a meta-analysis. Environ. Health Perspect 131, 56001. [PubMed: 37141244]

Low EVL Miryoung ; Bauer Cici ; Fisher-Hoch Susan P. ; Mccormick Joseph B. ; Abughosh Susan ; Essien Ekere J. ; Rodriguez Jessica ; Chen Hua. 2022. Association of puberty stage and weight status with cardiometabolic risk in children and adolescents living on the texas-mexico border. 20:440–450.

Luu HH, Song WX, Luo X, Manning D, Luo J, Deng ZL, et al. , 2007. Distinct roles of bone morphogenetic proteins in osteogenic differentiation of mesenchymal stem cells. J. Orthop. Res 25, 665–677. [PubMed: 17290432]

Marshall WA, Tanner JM, 1969. Variations in pattern of pubertal changes in girls. Arch. Dis. Child 44, 291–303. [PubMed: 5785179]

Marshall WA, Tanner JM, 1970. Variations in the pattern of pubertal changes in boys. Arch. Dis. Child 45, 13–23. [PubMed: 5440182]

Mederle OA, Balas M, Ioanoviciu SD, Gurban CV, Tudor A, Borza C, 2018. Correlations between bone turnover markers, serum magnesium and bone mass density in postmenopausal osteoporosis. Clin. Interv. Aging 13, 1383–1389. [PubMed: 30122910]

Moran A, Jacobs DR Jr., Steinberger J, Ching-Ping H, et al. , 1999. Insulin resistance during puberty: results from clamp studies in 357 children. Diabetes 48, 2039–2044. [PubMed: 10512371]

Mostafa S, Pakvasa M, Coalson E, Zhu A, Alverdy A, Castillo H, et al. , 2019. The wonders of bmp9: from mesenchymal stem cell differentiation, angiogenesis, neurogenesis, tumorigenesis, and metabolism to regenerative medicine. Genes & Diseases 6, 201–223. [PubMed: 32042861]

Nicole W, 2020. Breaking it down: estimating short-chain pfas half-lives in a human population. Environ. Health Perspect 128, 114002. [PubMed: 33174763]

NTP. 2016. Ntp monograph: Immunotoxicity associated with exposure to perfluorooctanoic acid (pfoa) or perfluorooctane sulfonate (pfos). Research Triangle Park, NC:U.S. Department of Health and Human Services, Office of Health Assessment and Translation.

Pan HT, Xiong YM, Zhu HD, Shi XL, Yu B, Ding HG, et al. , 2022. Proteomics and bioinformatics analysis of cardiovascular related proteins in offspring exposed to gestational diabetes mellitus. Frontiers in Cardiovascular Medicine 9, 1021112. [PubMed: 36277748]

Pan K, Xu J, Long X, Yang L, Huang Z, Yu J, 2023. The relationship between perfluoroalkyl substances and hypertension: a systematic review and meta-analysis. Environ Res 232, 116362.

Pennings JLA, Jennen DGJ, Nygaard UC, Namork E, Haug LS, van Loveren H, et al. , 2016. Cord blood gene expression supports that prenatal exposure to perfluoroalkyl substances causes depressed immune functionality in early childhood. J. Immunotoxicol 13, 173–180. [PubMed: 25812627]

Qu J, Zhao Y, Zhang L, Hu S, Liao K, Zhao M, et al. 2022. Evaluated serum perfluoroalkyl acids and their relationships with the incidence of rheumatoid arthritis in the general population in hangzhou, china. Environmental pollution (Barking, Essex : 1987) 307:119505.

Rochette L, Dogon G, Zeller M, Cottin Y, Vergely C. 2021. Gdf15 and cardiac cells: Current concepts and new insights. International journal of molecular sciences 22.

Rudzanová B, Thon V, Vespalcová H, Martyniuk CJ, Piler P, Zvona M, et al. , 2024. Altered transcriptome response in pbmcs of czech adults linked to multiple pfas exposure: B cell development as a target of pfas immunotoxicity. Environ. Sci. Tech 58, 90–98.

Salihovic S, Lind L, Larsson A, Lind PM, 2020. Plasma perfluoroalkyls are associated with decreased levels of proteomic inflammatory markers in a cross-sectional study of an elderly population. Environ. Int 145, 106099. [PubMed: 32916415]

Sevillano J, Sánchez-Alonso MG, Pizarro-Delgado J, Ramos-Álvarez MDP. 2021. Role of receptor protein tyrosine phosphatases (rptps) in insulin signaling and secretion. International journal of molecular sciences 22.

Shaw N, Högler W, 2012. Chapter 15 - biochemical markers of bone metabolism. In: Pettifor JM, Jüppner H. (Eds.), Pediatric Bone (second Edition), (glorieux FH. Academic Press, San Diego, pp. 361–381.

Si J, Wang C, Zhang D, Wang B, Zhou Y, 2020. Osteopontin in bone metabolism and bone diseases. Medical Science Monitor : International Medical Journal of Experimental and Clinical Research 26, e919159.

Steenland K, Zhao L, Winquist A, Parks C, 2013. Ulcerative colitis and perfluorooctanoic acid (pfoa) in a highly exposed population of community residents and workers in the mid-ohio valley. Environ. Health Perspect 121, 900–905. [PubMed: 23735465]

Su JH, Luo MY, Liang N, Gong SX, Chen W, Huang WQ, et al. , 2021. Interleukin-6: a novel target for cardio-cerebrovascular diseases. Front. Pharmacol 12, 745061.

Sun X, Yang X, Zhang Y, Liu Y, Xiao F, Guo H, et al. , 2024. Correlation analysis between per-fluoroalkyl and poly-fluoroalkyl substances exposure and depressive symptoms in adults: nhanes 2005–2018. Sci. Total Environ 906, 167639.

Szilagyi JT, Avula V, Fry RC, 2020. Perfluoroalkyl substances (pfas) and their effects on the placenta, pregnancy, and child development: a potential mechanistic role for placental peroxisome proliferator–activated receptors (ppars). Current Environmental Health Reports 7, 222–230. [PubMed: 32812200]

Szklarczyk D, Gable AL, Lyon D, Junge A, Wyder S, Huerta-Cepas J, et al. , 2018. String v11: protein–protein association networks with increased coverage, supporting functional discovery in genome-wide experimental datasets. Nucleic Acids Res. 47, D607–D613.

Tang N, Song WX, Luo J, Luo X, Chen J, Sharff KA, et al. , 2009. Bmp-9-induced osteogenic differentiation of mesenchymal progenitors requires functional canonical wnt/beta-catenin signalling. J. Cell Mol. Med 13, 2448–2464. [PubMed: 19175684]

Thomas SJ, Snowden JA, Zeidler MP, Danson SJ, 2015. The role of jak/stat signalling in the pathogenesis, prognosis and treatment of solid tumours. Br. J. Cancer 113, 365–371. [PubMed: 26151455]

Tibshirani R, Walther G, Hastie T, 2002. Estimating the number of clusters in a data set via the gap statistic. J. R. Stat. Soc. Ser. B Stat Methodol 63, 411–423.

Tobisch B, Blatniczky L, Barkai L, 2015. Cardiometabolic Risk Factors and Insulin Resistance in Obese Children and Adolescents: Relation to Puberty. 10, 37–44.

von Holst H, Nayak P, Dembek Z, Buehler S, Echeverria D, Fallacara D, et al. , 2021. Perfluoroalkyl substances exposure and immunity, allergic response, infection, and asthma in children: review of epidemiologic studies. Heliyon 7, e08160.

Wagner N, Wagner KD, 2020. The role of ppars in disease. Cells 9.

Wanby P, Nobin R, Von SP, Brudin L, Carlsson M, 2016. Serum levels of the bone turnover markers dickkopf-1, sclerostin, osteoprotegerin, osteopontin, osteocalcin and 25-hydroxyvitamin d in swedish geriatric patients aged 75 years or older with a fresh hip fracture and in healthy controls. J. Endocrinol. Invest 39, 855–863. [PubMed: 26850415]

Wang D, Uhrin P, Mocan A, Waltenberger B, Breuss JM, Tewari D, et al. , 2018. Vascular smooth muscle cell proliferation as a therapeutic target. Part 1: Molecular targets and pathways. Biotechnol. Adv 36, 1586–1607. [PubMed: 29684502]

Wen S-H, Lu Z-S, 2011. Factors affecting the effective number of tests in genetic association studies: a comparative study of three pca-based methods. J. Hum. Genet 56, 428–435. [PubMed: 21451529]

Wiromrat P, Rattanathongkom A, Laoaroon N, Suwannaying K, Komwilaisak P, Panamonta O, et al. , 2023. Bone mineral density and dickkopf-1 in adolescents with non-deletional hemoglobin h disease. J. Clin. Densitom 26, 101379.

Zabolotny JM, Kim YB, Peroni OD, Kim JK, Pani MA, Boss O, et al. , 2001. Overexpression of the lar (leukocyte antigen-related) protein-tyrosine phosphatase in muscle causes insulin resistance. PNAS 98, 5187–5192. [PubMed: 11309481]

Zhang Y, Wang Y, Li X, Zhang J, Mao J, Li Z, et al. , 2004. The lrp5 high-bone-mass g171v mutation disrupts lrp5 interaction with mesd. Mol. Cell. Biol 24, 4677–4684. [PubMed: 15143163]

Zhao Y, Jin H, Qu J, Zhang S, Hu S, Xue J, et al. , 2022. The influences of perfluoroalkyl substances on the rheumatoid arthritis clinic. BMC Immunol. 23, 10. [PubMed: 35246023]

Zota AR, Geller RJ, Romano LE, Coleman-Phox K, Adler NE, Parry E, et al. , 2018. Association between persistent endocrine-disrupting chemicals (pbdes, oh-pbdes, pcbs, and pfass) and

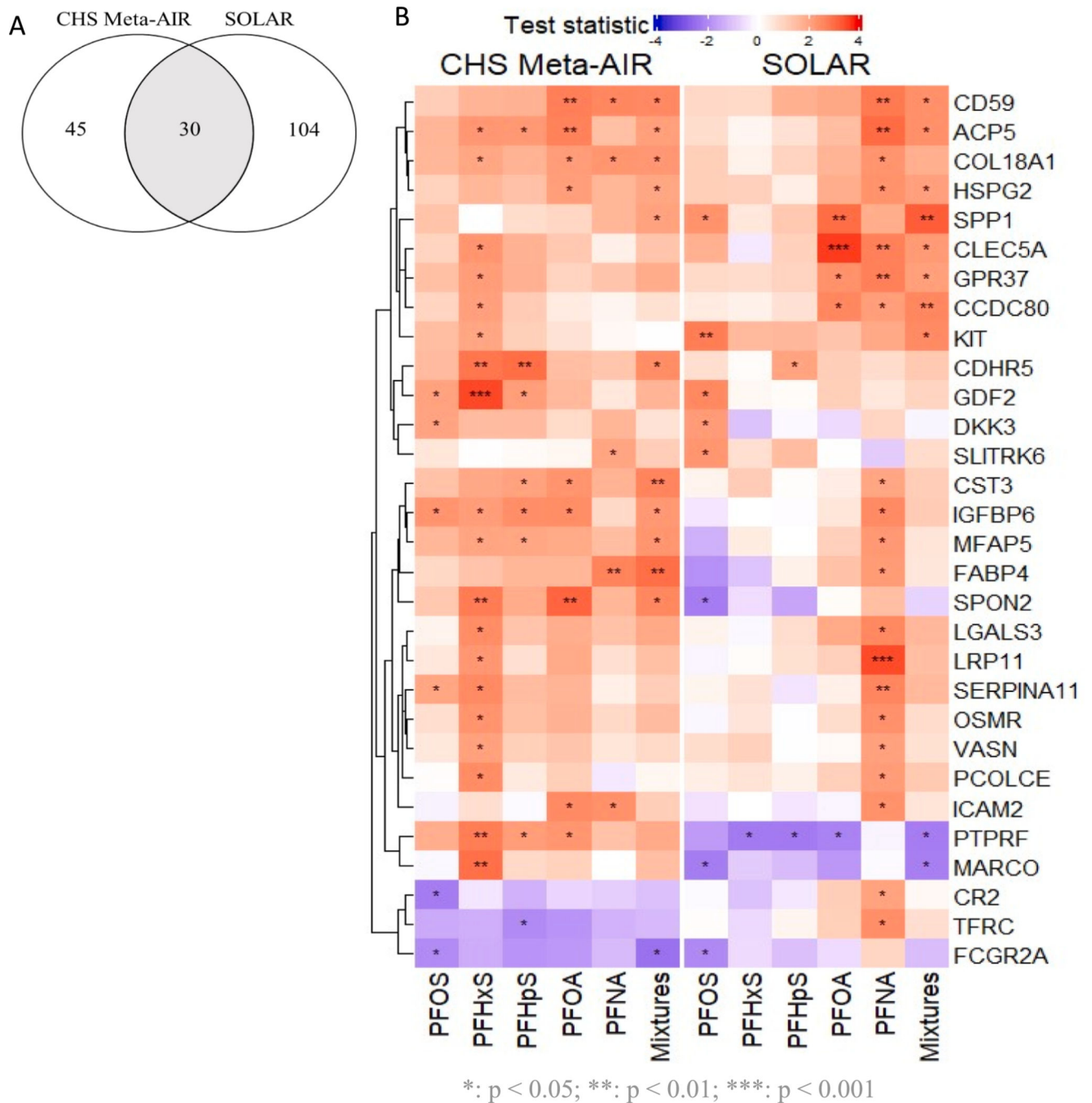biomarkers of inflammation and cellular aging during pregnancy and postpartum. Environ. Int 115, 9–20. [PubMed: 29533840]

Fig. 1.
Exploratory analysis of shared PFAS-protein associations in SOLAR and Meta-AIR ($p <$
0.05). (A) Number of overlapped proteins in two cohorts ($n = 30$ proteins). (B) Heatmap
showing the associations between PFAS and shared proteins.

Table 1

Baseline characteristics of participants in SOLAR (2001–2012) and Meta-AIR (2014–2018).

General Characteristics	SOLAR	Meta-AIR	*p*-value
Sample size	312	137	N/A
Age, years [mean ± *SD*]	11.3 ± 1.7	19.9 ± 1.3	N/A
Sex, Female [*n* (%)]	133 (43)	61 (45)	0.79
BMI, kg/m^2 [mean ± *SD*]	28.2 ± 5.8	29.6 ± 4.7	< 0.01
Obesity[1] [*n* (%)]	247 (79)	48 (35)	
Ethnicity [*n* (%)] Hispanic	312 (100)	79 (58)	< 0.001
Non-Hispanic	0 (0)	58 (42)	
Study Wave [*n* (%)]			
Wave 1 (2001–2003)	234 (75)	N/A	N/A
Wave 2 (2010–2012)	78 (25)	N/A	
Socioeconomic Status [*n* (%)]			
Modified Hollingshead Four-Factor Index			
[3, 11]	68 (22)	N/A	N/A
(11, 15.5]	67 (22)	N/A	
(15.5, 22]	71 (23)	N/A	
(22, 63.5]	71 (23)	N/A	
Missing	35 (11)	N/A	
Household Education Level < High School	146 (47)	25 (18)	< 0.001
High School Graduate	89 (29)	17 (12)	
> High School	43 (14)	91 (66)	
Missing	34 (11)	4 (3)	
Puberty Status [*n* (%)]			
Pre-puberty Tanner stage 1	99 (32)	N/A	N/A
Puberty Tanner stage 2	114 (37)	N/A	
Puberty Tanner stage 3	42 (14)	N/A	
Puberty Tanner stage 4	37 (12)	N/A	
Post-puberty Tanner stage 5	20 (6)	N/A	

Obesity is defined as a BMI 95th percentile for age and sex in SOLAR and a BMI 30 kg/m^2 in Meta-AIR.

Note: *p*-values not reported for variables that were only measured in one cohort.

N/A, not applicable.

Table 2

Geometric mean and 95% confidence intervals of PFAS concentrations (μg/L) in overweight and obese adolescents from SOLAR, and young adults from Meta-AIR, compared to adolescents from the National Health and Nutrition Examination Survey (NHANES) years 2007–2008 and 2017–2018.

PFAS Sub-class	PFAS Name	SOLAR 2001–12	Meta-AIR 2014–18	NHANES Serum PFAS concentrations, Age 12–19 years	
				Survey (Years): 2007–08	Survey (Years): 2017–18
PFSAs	PFOS	11.8 (10.8, 12.9)	3.31 (3.06, 3.58)	11.3 (10.3, 12.3)	2.68 (2.31, 3.12)
	PFHxS	1.44 (1.34, 1.56)	1.05 (0.92, 1.19)	2.40 (2.09, 2.75)	0.87 (0.73, 1.02)
	PFHpS	0.37 (0.35, 0.40)	0.18 (0.17, 0.19)	N.R.	0.15 (0.12, 0.20)
PFCAs	PFOA	3.29 (3.09, 3.50)	1.34 (1.26, 1.42)	3.91 (3.71, 4.12)	1.42 (1.33, 1.52)
	PFNA	0.59 (0.57, 0.61)	0.48 (0.46, 0.50)	1.16 (1.04, 1.30)	0.35 (0.29, 0.42)

Abbreviations: PFSAs: perfluorosulfonic acids; PFCAs: perfluorocarboxylic acids; N.R.: not reported

Table 3

Significant PFAS-protein associations, adjusting for covariates and multiple comparisons in SOLAR, and cross-database protein functional annotations.

Protein names	Model 1[a] β (95 % CI)	Model 2[b] β (95 % CI)	Protein functional annotations
PFOS (3 proteins)			
BPIFB1	0.27 (0.11, 0.42)[*]	0.25 (0.09, 0.40)	Innate immunity in the respiratory system
CLUL1	0.25 (0.10, 0.39)[*]	0.24 (0.10, 0.38)[*]	(Unknown)
NCAM1	0.13 (0.06, 0.21)[*]	0.13 (0.06, 0.21)[*]	Nervous system development; immune surveillance
PFOA (3 proteins)			
CLEC5A	0.14 (0.07, 0.21)[*]	0.13 (0.06, 0.20)[*]	Osteoclastogenesis; pro-inflammation; immune response
RNASE3	0.75 (0.31, 1.19)[*]	0.76 (0.32, 1.21)[*]	Antimicrobial peptides; asthma
HMOX1	0.25 (0.12, 0.38)[*]	0.24 (0.11, 0.38)[*]	Heme catabolism; response to stress
PFHpS (1 protein)			
SSC4D	0.66 (0.28, 1.03)[*]	0.61 (0.24, 0.99)	Immune response
PFNA (7 proteins)			
ACP5	0.14 (0.06, 0.23)[*]	0.13 (0.06, 0.22)	Osteopontin; osteoclast differentiation; rheumatoid arthritis
CLEC1A	0.17 (0.07, 0.27)[*]	0.18 (0.08, 0.29)[*]	Regulation of dendritic cell function; inflammation
HMOX1	0.34 (0.18, 0.51)[*]	0.34 (0.18, 0.51)[*]	Heme catabolism; response to stress
LRP11	0.18 (0.07, 0.29)[*]	0.19 (0.08, 0.30)[*]	Phosphoprotein binding activity
MCAM	0.19 (0.07, 0.30)[*]	0.17 (0.06, 0.28)	Angiogenesis; biomarker of chronic obstructive pulmonary disease and uveal melanoma.
SPARCL1	0.19 (0.08, 0.29)[*]	0.17 (0.06, 0.27)	Extracellular matrix binding; regulation of insulin-like growth factor transport
SSC5D	0.26 (0.12, 0.40)[*]	0.27 (0.13, 0.41)[*]	Innate defense; regulation of interleukin-8 production
Tertiles of PFAS Mixtures (1 protein)			
SSC5D	0.24 (0.10, 0.38)[*]	0.24 (0.10, 0.38)[*]	Innate defense; regulation of interleukin-8 production

Protein abbreviations: BPI fold containing family B member 1 (BPIFB1); Clusterin-like protein 1 (CLUL1); Neural cell adhesion molecule 1 (NCAM1); C-type lectin domain containing 5A (CLEC5A); Eosinophil cationic protein (RNASE3); Heme oxygenase 1 (HMOX1); Scavenger receptor cysteine-rich domain-containing group B protein (SSC4D); Acid phosphatase 5, tartrate resistant (ACP5); C-type lectin domain family 1 member A (CLEC1A); Low-density lipoprotein receptor-related protein 11 (LRP11); Melanoma cell adhesion molecule (MCAM); SPARC like 1 (SPARCL1); Scavenger receptor cysteine rich family member with 5 domains (SSC5D).

[a]Model 1 adjusted for age, sex, study wave, and socioeconomic status (SES).

[b]Model 2 additionally adjusted for tanner stage.

[*]Statistical significance for multiple comparisons based on a PCA-adjusted α threshold of 0.00128.

Table 4

Significant PFAS-protein associations, adjusting for covariates and multiple comparisons in Meta-AIR, and cross-database protein functional annotations.

Protein names	β (95 % CI)[a]	Functional annotations
PFOA (1 protein)		
LBP	0.42 (0.17, 0.67)[*]	Innate immunity
PFHxS (2 proteins)		
GDF2	0.12 (0.05, 0.19)[*]	Inhibitor of angiogenesis; cartilage and bone development; differentiation of cholinergic central nervous system neurons
PRSS2	0.15 (0.06, 0.23)[*]	Defensin processing in the ileum; Pancreatic secretion; collagen degradation
PFNA (1 protein)		
AOC3	−0.25 (−0.41, −0.10)[*]	Monoamine oxidase activity; adipogenesis
Tertiles of PFAS Mixtures (3 proteins)		
AOC3	−0.16 (−0.26, −0.07)[*]	Monoamine oxidase activity; adipogenesis
GDF15	0.18 (0.08, 0.28)[*]	Pleiotropic cytokine; stress response after cellular injury; inflammation; oxidative stress
IL6	0.43 (0.18, 0.69)[*]	Inflammation; immunity; tissue regeneration; metabolism

Protein abbreviations: Lipopolysaccharide-binding protein (LBP); Growth/differentiation factor 2 (GDF2); Trypsin-2 (PRSS2); Amine oxidase copper containing 3 (AOC3); Growth differentiation factor 15 (GDF15); Interleukin-6 (IL6).

[*] Statistical significance for multiple comparisons based on a PCA-adjusted α threshold of 0.00178.

[a] Model adjusted for age, sex, and parental education.